TU Delft

Delft University of Technology

Active Disturbance Rejection Control for Uncertain Nonlinear Systems With Sporadic Measurements

He, Kanghui; Dong, Chaoyang; Wang, Qing

DOI
10.1109/JAS.2022.105566

Publication date
2022

Document Version
Final published version

Published in
IEEE/CAA Journal of Automatica Sinica

Citation (APA)
He, K., Dong, C., & Wang, Q. (2022). Active Disturbance Rejection Control for Uncertain Nonlinear Systems With Sporadic Measurements. *IEEE/CAA Journal of Automatica Sinica*, *9*(5), 893-906. https://doi.org/10.1109/JAS.2022.105566

Important note
To cite this publication, please use the final published version (if applicable).
Please check the document version above.

Copyright
Other than for strictly personal use, it is not permitted to download, forward or distribute the text or part of it, without the consent of the author(s) and/or copyright holder(s), unless the work is under an open content license such as Creative Commons.

Takedown policy
Please contact us and provide details if you believe this document breaches copyrights.
We will remove access to the work immediately and investigate your claim.

This work is downloaded from Delft University of Technology.
For technical reasons the number of authors shown on this cover page is limited to a maximum of 10.

Green Open Access added to TU Delft Institutional Repository

'You share, we take care!' - Taverne project

https://www.openaccess.nl/en/you-share-we-take-care

Otherwise as indicated in the copyright section: the publisher is the copyright holder of this work and the author uses the Dutch legislation to make this work public.

Active Disturbance Rejection Control for Uncertain Nonlinear Systems With Sporadic Measurements

Kanghui He, *Student Member, IEEE*, Chaoyang Dong, and Qing Wang

***Abstract*—This paper deals with the problem of active disturbance rejection control (ADRC) design for a class of uncertain nonlinear systems with sporadic measurements. A novel extended state observer (ESO) is designed in a cascade form consisting of a continuous time estimator, a continuous observation error predictor, and a reset compensator. The proposed ESO estimates not only the system state but also the total uncertainty, which may include the effects of the external perturbation, the parametric uncertainty, and the unknown nonlinear dynamics. Such a reset compensator, whose state is reset to zero whenever a new measurement arrives, is used to calibrate the predictor. Due to the cascade structure, the resulting error dynamics system is presented in a non-hybrid form, and accordingly, analyzed in a general sampled-data system framework. Based on the output of the ESO, a continuous ADRC law is then developed. The convergence of the resulting closed-loop system is proved under given conditions. Two numerical simulations demonstrate the effectiveness of the proposed control method.**

***Index Terms*—Active disturbance rejection control (ADRC), extended state observer (ESO), sampled measurements, uncertain nonlinear systems.**

I. Introduction

THE issue of controlling systems subject to uncertainties has received considerable attention over the past decades because system uncertainties, such as external disturbances [1], un-modeled dynamics [2], and parametric uncertainties [3] are inevitably introduced in many practical systems. As a rising control technology, the active disturbance rejection control (ADRC), which was first proposed by Han [4], is an innovative and effective strategy to cope with uncertainties appearing in the nonlinear systems. The most distinctive feature of the ADRC is the estimation and compensation strategy. As an almost model-free control scheme, ADRC avoids the tedious task of establishing an accurate system mathematical model and improves the anti-interference capability of the control system. Because of these outstanding performance advantages, ADRC has been successfully employed in a broad range of practical engineering problems, such as motorbicycles [5], unmanned aerial vehicles [6], and flexible manipulators [7].

However, the structure of ADRC proposed by Han is complex, which makes rigorous stability analysis for ADRC face significant challenges and fall behind its extensive application. To overcome this obstacle, the work in [8] has developed a linear ADRC structure in which the controller and the observer are both presented in linear forms with one parameter: bandwidth, to be tuned. In [9], the exponential convergence of linear ADRC was systematically analyzed based on singular perturbation theories. Meanwhile, the nonlinear ADRC for single-input-single-output (SISO) systems was first reported by Guo and Zhao in [10], and then extended to multiple-input-multiple-output (MIMO) systems in [11]. After that, literature has emerged that comprising an extended state observer (ESO) and a projected gradient estimator makes the ADRC scheme incorporate no prior knowledge of control coefficient [12]. More recently, in [13], an unconventional ADRC approach was proposed for a class of uncertain time-delay systems, utilizing a modified ESO to predict future states of plants. Works on the learning-based ADRC design can be found in [14].

In other aspects, control design for plants with sampled measurements, which is encountered in most physical systems, has been extensively explored in recent literature. In most control systems, information is usually transmitted in the form of digital signals. Because of communication constraints between networks, sensors may not be able to broadcast data continuously or periodically. The loss of information in sampling intervals may lead to degradation of the control performance and even instability of the overall system. Therefore, control design and analysis for systems with discrete nature of the available outputs have attracted worldwide attention, especially in the fields of fuzzy control [15], H_∞ control [16], and some observer-based control techniques [17]. Unfortunately, there are almost no related researches on ADRC design and analysis for systems with intermittent measurement information. The main challenge lies in the fact that the conventional ESO is sensitive to measurement variation and will lose the estimation ability under the discontinuous measurement information. Moreover, the introduction of sporadic measurements induces the error dynamic in a hybrid form, thus making the analysis of the

Manuscript received June 11, 2021; revised July 24, 2021 and October 22, 2021; accepted November 20, 2021. This work was supported by the National Natural Science Foundation of China (61833016, 61873295). Recommended by Associate Editor Weinan Gao. *(Corresponding author: Chaoyang Dong.)*

Citation: K. H. He, C. Y. Dong, and Q. Wang, " Active disturbance rejection control for uncertain nonlinear systems with sporadic measurements," *IEEE/CAA J. Autom. Sinica*, vol. 9, no. 5, pp. 893–906, May 2022.

K. H. He was with the School of Aeronautic Science and Engineering, Beihang University, Beijing 100191, China. He is now with the Delft Center for System and Control, Delft University of Technology, Delft, the Netherlands (e-mail: k.he@tudelft.nl).

C. Y. Dong is with the School of Aeronautic Science and Engineering, Beihang University, Beijing 100191, China (e-mail: dongchaoyang@buaa.edu.cn).

Q. Wang is with the School of Automation Science and Electrical Engineering, Beihang University, Beijing 100191, China (e-mail: wangqing@buaa.edu.cn).

Color versions of one or more of the figures in this paper are available online at http://ieeexplore.ieee.org.

Digital Object Identifier 10.1109/JAS.2022.105566

Authorized licensed use limited to: TU Delft Library. Downloaded on February 02,2023 at 10:39:32 UTC from IEEE Xplore. Restrictions apply.

stability of the observer and the closed-loop system more difficult and complicated.

On the other hand, it should be recognized that state estimation techniques with sporadically available measurements have been extensively explored in recent literature. The approaches essentially belong to two main families. The first one is the so-called continuous-discrete time observer whose state is impulsive and reset at the arrival of a new measurement. The design and analysis of such an observer are reported, e.g., in [18]–[23]. Specifically, the work in [18] considers the observation of linear systems with unknown parameters and discrete time measurements. To mitigate the effect of parametric uncertainty, the structure of the proposed observer is multilayered consisting of the extended Kalman filter and adaptive estimation method. Later, the methodology in [18] is extended to a more general nonlinear system in [22]. What is more, the high gain impulsive observer design for the Lipschitz nonlinear systems is also pursued in [19]. The second family is the continuous time observer whose observation error is estimated synchronously by a continuous- discrete time predictor. Related works can be seen in [24]–[29]. In particular, the authors in [24] provide a methodology of observer redesign from continuous sampling systems to intermittent sampling systems. A different method is investigated in [26], where the exponential stability results for a class of sampled-data systems are obtained and the established stability results can provide a guideline for the implementation of observer design based on isolated time measurements. However, we should point out that the methods mentioned above are only suitable for linear systems [18], or require some prior knowledge of nonlinear dynamics. For instance, the nonlinear part is completely known [19]–[21], [24], [26], [27], the nonlinear function is Lipschitz [20], [23], [25], [28]. More importantly, no attempt is made in the overall estimation of nonlinear uncertainty, which is sometimes demanded in control devices such as the feedback linearization technique.

Motivated by these observations, in this paper we consider the ADRC design for a class of nonlinear systems with periodically sampled outputs. First, a redesign procedure is made to develop a predictor-based continuous time ESO whose state consists of the estimations of both system state and the total uncertainty. Then, an approximate feedback linearization control law accounting for peaking phenomena is presented. Theoretical analysis and numerical simulations suggest that the lower bound of the ESO gain is restricted by the sampling interval. This is a new feature compared with most previous ADRC results. The main contributions of this article are twofold:

1) To our best knowledge, this paper is the first attempt of ADRC application in sporadic-in-measurement systems. The structure of the proposed ADRC is developed, in which a predictor-based continuous time ESO executes state and uncertainty estimation based on intermittent measurements.

2) Differently from all existing estimation techniques for systems with sampled measurements [18]–[29], the ESO proposed in this paper does not contain any impulsive motion in either state estimation or observation error prediction, and more significantly, eliminates some restriction on the system nonlinearity.

The remainder of this paper is organized as follows. In Section II, the control problem and objective are formulated and some important assumptions are listed. The observer and controller design is presented in Section III. In Section IV we focus on the stability analysis of the ESO and give some results on a class of more general sampled-data systems. Section V gives main results on the closed-loop system. After that, the effectiveness of the proposed method is discussed through two examples in Section VI. Finally, we conclude this paper and discuss some prospective research in Section VII.

Notations: The set $\mathbb{N}$ denotes the set of positive integers containing zero while the set $\mathbb{N}^+$ is the set of strictly positive integers. The set $\mathbb{R}^+$ is the set of positive reals while the set $\mathbb{R}^{m\times n}$ denotes the set of $m\times n$-dimensional matrices. The identity matrix with dimension $n\times n$ is written as I_n. The Euclidean norm of a vector is denoted as $\|\cdot\|$. $\nabla f(\cdot)$ represents the gradient of a function $f(\cdot)$. We utilize C to represent the set of all continuously differentiable functions. A function $\beta(\cdot):[0,\infty)\to[0,\infty)$ is called to belong to a class of K_∞ functions only if $\beta(\cdot)$ is continuous and strictly increasing with $\beta(0)=0$ and $\beta(\infty)=\infty$. $\lambda_{P,\max}$ and $\lambda_{P,\min}$ represent the maximum and minimum eigenvalues of a symmetric positive definite matrix P respectively, and $\ell_P=\lambda_{P,\max}/\lambda_{P,\min}$ denotes P's conditioning number. $O(\mu)$ refers to the equivalent infinitesimal notation of a small positive real number μ.

II. Preliminaries

A. Problem Formulation

Consider the following nonlinear system with sporadic measurements:

$$\begin{cases}\dot z(t)=f_0(t,x(t),z(t),\omega(t))\\ \dot x(t)=Ax(t)+B[f(t,x(t),z(t),\omega(t))\\ \qquad\quad +g(t,x(t),z(t),\omega(t))u(t)]\\ y(t_k)=Cx(t_k),t\ge t_0,\ \ k\in\mathbb{N}\end{cases}\tag{1}$$

where $x(t)=[x_1(t),\dots,x_n(t)]^T\in\mathbb{R}^n$ and $z(t)\in\mathbb{R}^p$ are the state vectors, $\dot z(t)=f_0(t,x(t),z(t),\omega(t))$ is the zero dynamics of the system, $\omega\in\mathbb{R}$ is the external disturbance, $u(t)\in\mathbb{R}$ is the input signal, $y(t_k)\in\mathbb{R}$ is the sampled output at time instant t_k, $\tau_k=t_{k+1}-t_k>0$ is the time-varying sampling period, $f_0(\cdot)\in C([t_0,\infty]\times\mathbb{R}^{n+p+1},\mathbb{R}^p)$, $f(\cdot)$, $g(\cdot)\in C([t_0,\infty]\times\mathbb{R}^{n+p+1},\mathbb{R})$ are unknown nonlinear functions, and the triple matrices $(A,\ B,\ C)$ represent a chain of n-dimensional integrators

$$A=\begin{bmatrix}0&1&0&\cdots&0\\0&0&1&\cdots&0\\\vdots&\vdots&\vdots&\ddots&\vdots\\0&0&0&\cdots&1\\0&0&0&\cdots&0\end{bmatrix}\in\mathbb{R}^{n\times n},\ B=\begin{bmatrix}0\\0\\\vdots\\0\\1\end{bmatrix}\in\mathbb{R}^{n\times1}$$

$$C=[1\ 0\ \cdots\ 0]\in\mathbb{R}^{1\times n}.\tag{2}$$

It is worth mentioning that the dynamics of many practical engineering systems can be described by model (1) or can be

Authorized licensed use limited to: TU Delft Library. Downloaded on February 02,2023 at 10:39:32 UTC from IEEE Xplore. Restrictions apply.

transformed to (1), for instance, the biological systems [30], the urban traffic systems [31], and the hypersonic vehicle systems [32]. The sampled measurements modeled in this paper may result from the limited data transmission rate or event-triggered mechanisms in networked control systems, or from sensors' limited sampling frequency. The discrete nature of measurements can cause considerable damage to safety-critical systems in which real-time performance needs to be guaranteed. The conventional ADRC design for system (1) has been widely investigated in the absence of sporadic measurements. However, the ADRC technique can not be directly applied to (1) because the traditional ESO relies on the continuity of system output. The control objective of this paper is thereby to design the ADRC law to accommodate uncertain nonlinearities with limited knowledge of system measurements.

In this paper, $g(t,x(t),z(t),\omega(t))$ is assumed to be partially known and can be modeled as $g(t,x(t),z(t),\omega(t)) = g_0(x(t)) + g_\Delta(t,x(t),z(t),\omega(t))$. $g_0(\cdot) \in C(\mathbb{R}^n, \mathbb{R})$ is known, non-zero, and globally bounded, while $g_\Delta(\cdot) \in C([t_0,\infty]\times\mathbb{R}^{n+p+1}, \mathbb{R})$ is an unknown nonlinear part.

Throughout the paper, the original system (1) is assumed to satisfy the following assumptions.

Assumption 1 [33]: The external disturbance $\omega(t)$ and its time derivative are assumed to be bounded. What is more, there exists an unknown continuous and positive definite function $\varpi(x,z,\omega) \in C(\mathbb{R}^{n+p+1}, \mathbb{R}^+)$ such that for any $t \ge t_0$

$$|f(t,x,z,\omega)| + \|f_0(t,x,z,\omega)\| + \|\nabla f(t,x,z,\omega)\| + \|\nabla f_0(t,x,z,\omega)\| \le \varpi(x,z,\omega).$$

Assumption 2 [33]: There exists a continuous, positive definite and radially unbounded function $V_0(z) \in C(\mathbb{R}^p, \mathbb{R}^+)$ such that for any $(t,x,z,\omega) \in [t_0, \infty)\times\mathbb{R}^{n+p+1}$

$$\frac{\partial V_0}{\partial z}(z) f_0(t,z,x,\omega) \le 0,\ \forall \|z\| \ge \beta_z(\|(x,\omega)\|)$$

where $\beta_z(\cdot)$ is a K_∞ function.

Assumption 3 [22]: The sampling intervals $\tau_k = t_{k+1} - t_k$, $k \in \mathbb{N}$ are bounded by $\tau_k \in [\tau_m, \tau_M]$, where τ_m and τ_M are positive constants.

Assumptions 1 and 2 can be commonly observed in the literature related to ADRC and can be verified for a series of practical control systems, including the inverted pendulum in [34]. Assumption 1 limits the unknown nonlinearities to a time-independent function, while Assumption 2 ensures that the zero dynamics with the input (t,x,ω) is bounded-input-bounded state (BIBS) stable. This condition is looser than that of the input-to-state stable (ISS) [12]. Besides, the assumption that the sampling interval is bounded is ubiquitous for control design in the presence of sporadic measurements.

B. Traditional ADRC

The predictor-based continuous time ESO to be designed later is issued from a proper redesign of the continuous ESO which has been extensively used in the estimation of nonlinear system's uncertainty. Before starting our design procedure, let us recall the conventional ADRC methodology for continuous-in-measurement systems. Notice that the system (1) is subjected to multiple uncertainties, including the uncertainty in zero dynamics $f_0(\cdot)$, the unmodeled dynamics $f(\cdot)$, the external disturbance ω, and the uncertainty of control coefficient $g_\Delta(\cdot)$. If the measurement equation in the original system (1) is in continuous form $y(t) = Cx(t)$, $t \ge t_0$, by defining the uncertain nonlinearity $f(t,x,z,\omega) + g_\Delta(t,x,z,\omega)u(t)$ as the extended state $x_{n+1}(t)$, we reconstruct (1) as follows:

$$\begin{cases} \dot z(t) = f_0(t,x(t),z(t),\omega(t)) \\ \dot x_1(t) = x_2(t) \\ \quad\vdots \\ \dot x_n(t) = x_{n+1}(t) + g_0(x(t))u(t) \\ \dot x_{n+1}(t) = h \\ y(t) = Cx(t),\ \ t \ge t_0. \end{cases} \tag{3}$$

Following the idea from [35], we can construct the following linear ESO to estimate the unmeasured states $x(t)$ and the total uncertainty $x_{n+1}(t)$.

$$\dot{\hat x}(t) = \bar A\hat x(t) + \bar B g_0(\hat x(t))u(t) + \frac{1}{\varepsilon^{n+1}}\Delta_\varepsilon^{-1} W(y(t) - \bar C\hat x(t)) \tag{4}$$

where $W = [w_1, w_2, \ldots, w_{n+1}]^T \in \mathbb{R}^{n+1}$ is designed such that the polynomial $s^{n+1} + w_1 s^n + \cdots + w_{n+1}$ is Hurwitz, $\Delta_\varepsilon = \mathrm{diag}\{1/\varepsilon^n, 1/\varepsilon^{n-1}, \ldots, 1\} \in \mathbb{R}^{(n+1)\times(n+1)}$, ε is a small parameter to be determined, $(\bar A, \bar C)$ is in the similar form with (A, C) in (2) where the dimension is changed to $n+1$, and $\bar B = [0, 0, \ldots, 1, 0]^T \in \mathbb{R}^{(n+1)\times 1}$.

The selection of the gain parameters W and ε is not only theoretically analyzed in [8] by using bandwidth theory but also investigated in practice, see for instance the work of [36]. In fact, if the parameter ε is selected small enough, the linear ESO (4) is essentially a high gain observer and more importantly, $\hat x_{n+1}(t)$ can be viewed as an appropriate estimate of the total uncertainty $x_{n+1}(t)$. According to Theorem 1 in [35], if $\dot x_{n+1}$ is bounded, there exist a series of constants σ_i and a finite time $T_1 > 0$ such that $|x_i(t) - \hat x_i(t)| \le \sigma_i$, $i = 1, 2, \ldots, n+1$, $\forall t \ge t_0 + T_1$. With this property, based on the output of the ESO (4) one can directly design the control law to approximately compensate the total uncertainty and stabilize the system near the equilibrium point.

In the sporadic-measurement-free case, the ESO (4) can be replaced by some other kinds of disturbance observers, such as high-order sliding mode observer (HOSMO) [37] and generalized proportional integral observer (GPIO) [38]. For systems with sporadic measurements, almost all the works concentrate on state estimation problems while no attempt has been made on the overall estimation of nonlinear uncertainty or disturbance.

III. Observer and Controller Design

In this paper, since the output measurements are available in a discrete manner, we redesign a predictor-based continuous time ESO for system (1) to derive the estimates of both the unmeasured states and total uncertainty.

$$\dot{\hat x}(t) = \bar A\hat x(t) + \bar B g_0(\hat x(t))u(t) + \frac{L\chi(t)}{\varepsilon},\quad \forall t \in [t_0, \infty) \tag{5}$$

Authorized licensed use limited to: TU Delft Library. Downloaded on February 02,2023 at 10:39:32 UTC from IEEE Xplore. Restrictions apply.

where $\hat{x}(t)=[\hat{x}_1(t),\ldots,\hat{x}_{n+1}(t)]^T\in\mathbb{R}^{n+1}$ represents the estimates of $x(t)$ and $x_{n+1}(t)$, $\chi(t)=[\chi_1(t),\ldots,\chi_{n+1}(t)]^T\in\mathbb{R}^{n+1}$ contains the approximation of observation error. ε is a small positive parameter to be designed later, and $L\in\mathbb{R}^{(n+1)\times(n+1)}$ is a diagonal matrix: $L=\text{diag}\{l_1,\ldots,l_{n+1}\}$.

In many recent works, the observation error in (5) is usually predicted by $\left(y(t_k)-\bar{C}\hat{x}(t_k)\right)e^{-l_1(t-t_k)}$, or directly given by $y(t_k)-\bar{C}\hat{x}(t_k)$. These approaches may induce cumulative error occurred in the sampling intervals. To this end, we develop an adaptive predictor to estimate the observation error. In particular, the vector variable $\chi(t)$ is updated through the following ordinary differential equation:

$$\dot{\chi}(t)=\frac{1}{\varepsilon}\bar{C}^T\left(\left(y(t_k)-\bar{C}\hat{x}(t_k)\right)e^{\frac{-l_1(t-t_k)}{\varepsilon}}+l_1\phi(t)\right)+\frac{1}{\varepsilon^2}\left(\bar{A}^T-\varepsilon Q\right)\chi(t)\ ,\ \forall t\in[t_0,\infty) \tag{6}$$

where $Q\in\mathbb{R}^{(n+1)\times(n+1)}$ is a diagonal matrix: $Q=\text{diag}\{q_1,\ldots,q_{n+1}\}$, and $\phi(t)\in\mathbb{R}$ is used to compensate for the adverse effects of cumulative errors and designed as

$$\phi(t)=\int_{t_k}^{t}\frac{1}{\varepsilon}\left(\left(y(t_k)-\bar{C}\hat{x}(t_k)\right)e^{\frac{-l_1(s-t_k)}{\varepsilon}}-\chi_1(s)\right)ds\quad t\in[t_0,\infty)\text{ with }\phi(t_k)=0. \tag{7}$$

It can be obviously seen that the proposed ESO is composed of three subsystems. The first subsystem is of $(n+1)$th order and is just a copy of the extended system with $x_{n+1}(t)=f(t,x(t),z(t),\omega(t))$. Due to the sampled output, the observation error term $y(t)-\bar{C}\hat{x}(t)$ in the continuous ESO is unavailable during sampling intervals $[t_k,\ t_{k+1})$. Therefore, we draw into the second subsystem as a predictor estimating the future observation error after a sampling instant. The state $\phi(t)$ in the last subsystem is generated through an integrator and is triggered to zero at sampling instants. The purpose of involving the last subsystem is to compensate the accumulated error during the sampling intervals.

Based on the output of the ESO (5)–(7), an output feedback linearization controller is given as

$$u_{\text{nom}}(t)=\frac{u_0(\bar{\hat{x}}_n)-\hat{x}_{n+1}}{g_0\left(\bar{\hat{x}}_n\right)} \tag{8}$$

where $\bar{\hat{x}}_n=[\hat{x}_1,\ldots,\hat{x}_n]^T$, and $u_0(\cdot)$ represents some kinds of linear or nonlinear feedback law which guarantees the globally asymptotic stability of the following n-dimensional chain of integrals:

$$\dot{x}(t)=Ax(t)+Bu_0(x).$$

Additionally, considering that peaking phenomena may occur due to the high gain property of the observer, we introduce a saturation version [39]

$$u(t)=Mg_\varepsilon\left(\frac{u_{\text{nom}}(t)}{M}\right) \tag{9}$$

to modify the original control input. $g_\varepsilon(\cdot)\in C(\mathbb{R},\mathbb{R})$ is a non-decreasing, odd, continuously differentiable function defined by

$$g_\varepsilon(r)=\begin{cases}r, & 0\le r\le 1\\ r+\dfrac{r-1}{\varepsilon}-\dfrac{r^2-1}{2\varepsilon}, & 1<r\le 1+\varepsilon\\ 1+\dfrac{\varepsilon}{2}, & r>1+\varepsilon.\end{cases} \tag{10}$$

M is a saturation bound to be designed later. Generally, the saturation bound should be selected such that the saturation function $g_\varepsilon(\cdot)$ will always work in the linear zone under state feedback [34].

The control framework is illustrated in Fig. 1.

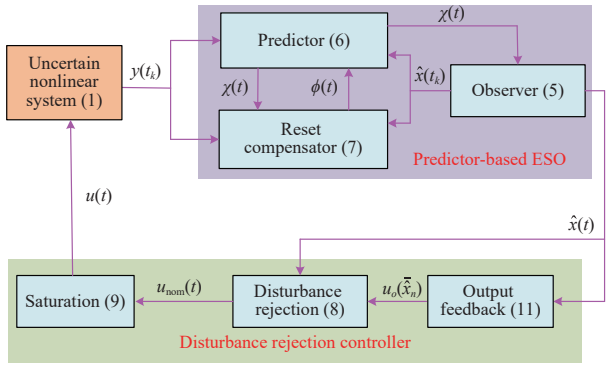

Fig. 1. The architecture of the proposed ESO and the disturbance rejection controller.

The following assumptions are made on the control $u_0(\cdot)$ and the ESO (5)–(7).

Assumption 4: $u_0(\cdot)$ is a globally Lipschitz function. What is more, there exist a continuous, positive definite and radially unbounded function $V_1(\cdot)\in C(\mathbb{R}^n,\mathbb{R}^+)$ and positive constants α_1, β_1, c_{11}, and c_{12} such that

$$c_{11}\|x(t)\|^2\le V_1(x(t))\le c_{12}\|x(t)\|^2$$

$$\sum_{i=1}^{n-1}x_{i+1}(t)\frac{\partial V_1(x(t))}{\partial x_i(t)}+u_0(x(t))\frac{\partial V_1(x(t))}{\partial x_n(t)}\le-\alpha V_1(x(t))$$

$$\left|\frac{\partial V_1(x(t))}{\partial x_n(t)}\right|\le\beta_1\|x(t)\|$$

hold for all $t\ge t_0$.

Assumption 5: The gain parameters l_i and q_i, $i=1,2,\ldots,n+1$ are selected such that the matrix $A_\xi=\begin{bmatrix}\bar{A} & -L\\ \bar{C}^T\bar{C} & \bar{A}^T-Q\end{bmatrix}\in\mathbb{R}^{(2n+2)\times(2n+2)}$ is Hurwitz.

Based on Assumption 1, let $\omega(t)\in\mathcal{W},\forall t\in[t_0,\infty)$ for a compact set $\mathcal{W}\in\mathbb{R}$. Meanwhile, by Assumption 2, there exists a positive constant c_z such that the compact set $\mathcal{Z}=\{z\in\mathbb{R}^p;\|z\|\le c_z\}$ is a positive invariant set for the zero dynamics. For any given compact set $\mathcal{X}\in\mathbb{R}^n$, define a compact set $\mathcal{Y}$ by $\mathcal{Y}=\mathcal{X}\times\mathcal{Z}\times\mathcal{W}$.

Assumption 6: The known control gain coefficient $g_0(x)$ satisfies the property of

$$\max_{(x,z,\omega)\in\mathcal{Y},\bar{\hat{x}}_n\in\mathcal{X}}\left|\frac{g(\cdot)-g_0(x)}{g_0(\bar{\hat{x}}_n)}\right|=\gamma_g<1.$$

Remark 1: The simplest way to satisfy Assumption 4 is to make $u_0(\cdot)$ be a linear form

Authorized licensed use limited to: TU Delft Library. Downloaded on February 02,2023 at 10:39:32 UTC from IEEE Xplore. Restrictions apply.

$$u_0(x(t)) = Kx(t) \tag{11}$$

where $K = [k_1, k_2, \ldots, k_n] \in \mathbb{R}^{1\times n}$ is chosen such that the matrix $A + BK$ is Hurwitz. Such control (9) with the general linear ESO (4) is the so-called linear ADRC. Assumption 6 is a common assumption for the ESO-based or high-gain-observer-based controllers, which means that the modeled control coefficient $g_0(x)$ should not be too much far away from the real control coefficient $g(t, x(t), z(t), \omega(t))$. In addition, the satisfiability of Assumption 5 will be discussed in detail in the next section.

Remark 2: One aspect of the proposed predictor-based observer is that neither the observer nor the predictor is impulsive. The calibration of the predictor is achieved through a compensation signal obtained by a reset operator. In retrospect to the existing research on observer design for sampled-in-measurement systems, one can see that some observers, e.g., in [18]–[23] were totally impulsive while others, e.g., in [24]–[28] were continuous in estimates but used impulsive output predictors. In this sense, this paper is the first attempt to utilize not only continuous observers but also continuous predictors. Actually, it is in general difficult to tell which one performs better than the others. However, from the stability analysis point of view, thanks to the separation of the estimation process and impulsive correction process, the error dynamics of the proposed ESO avoids any jumping stage and is thus classified as a kind of non-hybrid system. This property renders the stability analysis and parameter design more convenient and intuitive.

The proposed predictor-based ESO shows superiority in the estimation of both unmeasured states and uncertainty. First, the developed method is applicable to the case when systems contain large uncertainties, while existing results [19]–[29] need full or partial knowledge of nonlinear dynamics. What is more, the developed method can also provide a continuous prediction of these uncertainties, which is appealing for feedback control design. On the other hand, compared with some other sample-data control methods derived from ADRC, such as the event-triggered ADRC proposed in [40], [41], our approach employs the power of a predictor (6) for the ESO design, in which the observation error is online estimated by $\chi(t)$ (shown in Fig. 1), while in [40], [41], it is fixed at $y(t_k) - \bar{C}\hat{x}(t_k)$ during the sampling intervals. As a result, the cumulative observation error can be effectively suppressed by our control scheme. What is more, the sampling instant t_k in [40], [41] is designed by the event-triggered mechanism. In comparison, our work focuses on the development of the ESO's structure so that it can be applicable for systems where the sampling interval is directly determined by physical factors such as network transmission rate or sensor sampling frequency.

However, the high-gain property of the ESO causes some converse effects. First, the estimation capability is limited by the minimum sampling frequency, especially when ε is selected to be small. This problem will be theoretically formulated in Theorem 2. The other problem is the eradication of the "peaking" of the ESO. Even though it can be eliminated through the modification of saturation in (9), the control performance may still be degraded if the systems are oversaturated [42]. Some other solutions such as selecting adaptive gains [36] can be utilized and need further investigation.

IV. Convergence of the ESO

The separation principle for nonlinear systems implies that the faster convergence of the observer should be guaranteed before obtaining the stability of the proposed ADRC. In this section the stability condition of the ESO under the circumstance of bounded closed-loop performance, summarized as Theorem 2, will be addressed. Before that, we first derive the error dynamics of the proposed ESO and find that it belongs to a more general nonlinear sampled-data system. Given this, we study the exponentially input-to-state stable (eISS) condition of the sampled-data system and state it as Theorem 1, which will be exploited to get the results of the ESO with some additional assumptions.

A. Error Dynamics Equation

We define the estimation error of the ESO as the following scale:

$$\eta(t) = [\eta_1(t), \ldots, \eta_{n+1}(t)]^T,\ \eta_i(t) = \frac{x_i(t) - \hat{x}_i(t)}{\varepsilon^{n+1-i}} \tag{12}$$

with $i = 1, 2, \ldots, n+1$. It follows from (1), (5)–(7) and (12) that the error dynamics can be specified as:

$$\dot{\eta}(t) = \frac{1}{\varepsilon}\bar{A}\eta(t) + \bar{B}g_\Delta(t, x, z, \omega)u(t) + \bar{D}h(t) - \frac{1}{\varepsilon}L\vartheta(t) \tag{13}$$

where $\vartheta(t) = \Delta_\varepsilon \chi(t) \in \mathbb{R}^{n+1}$ with $\Delta_\varepsilon = \text{diag}\{1/\varepsilon^n, 1/\varepsilon^{n-1}, \ldots, 1\} \in \mathbb{R}^{(n+1)\times(n+1)}$ defined in (4) and $\bar{D} = [0, 0, \ldots, 0, 1]^T \in \mathbb{R}^{(n+1)\times 1}$.

On other aspects, the dynamics of the scaled observation error $\vartheta(t)$ can be computed as

$$\begin{aligned}\dot{\vartheta}(t) = &\frac{1}{\varepsilon^2}\Delta_\varepsilon\left(\bar{A}^T - \varepsilon Q\right)\vartheta(t) \\ &+ \frac{1}{\varepsilon}\Delta_\varepsilon\bar{C}^T\left(\bar{C}\Delta_\varepsilon^{-1}\eta(t_k)e^{-\frac{l_1(t-t_k)}{\varepsilon}} + l_1\phi(t)\right).\end{aligned} \tag{14}$$

From the facts that $\Delta_\varepsilon\bar{C}^T\bar{C}\Delta_\varepsilon^{-1} = \bar{C}^T\bar{C}$, $\Delta_\varepsilon\bar{C}^T = \frac{1}{\varepsilon^n}\bar{C}^T$, and $\Delta_\varepsilon\bar{A}^T = \varepsilon\bar{A}^T\Delta_\varepsilon$, we obtain

$$\begin{aligned}\dot{\vartheta}(t) &= \frac{1}{\varepsilon}\left(\bar{A}^T - Q\right)\vartheta(t) + \frac{1}{\varepsilon}\bar{C}^T\bar{C}\eta(t_k)e^{-\frac{l_1(t-t_k)}{\varepsilon}} + \frac{l_1}{\varepsilon^{n+1}}\bar{C}^T\phi(t) \\ &= \frac{1}{\varepsilon}\left(\bar{A}^T - Q\right)\vartheta(t) + \frac{1}{\varepsilon}\bar{C}^T\bar{C}\eta(t) + \frac{1}{\varepsilon}\bar{C}^T\rho(t)\end{aligned} \tag{15}$$

where $\rho(t) = \bar{C}\eta(t_k)e^{-l_1(t-t_k)/\varepsilon} - \bar{C}\eta(t) + \frac{l_1}{\varepsilon^n}\phi(t) \in \mathbb{R}$. Note that $\bar{C}\eta(t_k) = \eta_1(t_k)$ and $\dot{\eta}_1(t) = \eta_2(t)/\varepsilon - l_1\vartheta_1(t)/\varepsilon^2$, so compute the derivative of $\rho(t)$ with respect to time, then we get

$$\begin{aligned}\dot{\rho}(t) = &-\frac{l_1}{\varepsilon}\eta_1(t_k)e^{-\frac{l_1(t-t_k)}{\varepsilon}} - \frac{1}{\varepsilon}\eta_2(t) + \frac{l_1}{\varepsilon}\vartheta_1(t) \\ &+ \frac{l_1}{\varepsilon^{n+1}}\left(\left(y(t_k) - \bar{C}\hat{x}(t_k)\right)e^{-\frac{l_1(t-t_k)}{\varepsilon}} - \chi_1\right) \\ = &-\frac{1}{\varepsilon}\eta_2(t).\end{aligned} \tag{16}$$

Authorized licensed use limited to: TU Delft Library. Downloaded on February 02,2023 at 10:39:32 UTC from IEEE Xplore. Restrictions apply.

A direct integral calculation shows that $\rho(t)$ can be expressed by the reset operator $\rho(t)=\Omega(\eta(t))$ with

$$\Omega:\begin{cases}\rho(t)=-\dfrac{1}{\varepsilon}\displaystyle\int_{t_k}^{t}\eta_2(s)ds,\ \ \forall t\neq t_k\\ \rho(t_k)=0.\end{cases}\tag{17}$$

Define the condensed state vector $\xi^T(t)=(\eta^T(t),\ \vartheta^T(t))$, then the scaled error dynamics of the ESO can be rewritten as

$$\dot{\xi}(t)=\frac{1}{\varepsilon}A_\xi\xi(t)+\begin{pmatrix}\bar{D}h(t)+\bar{B}g_\Delta u(t)\\ 0_{n+1,1}\end{pmatrix}+\frac{1}{\varepsilon}\begin{pmatrix}0_{n+1,1}\\ \bar{C}^T\rho(t)\end{pmatrix}\tag{18}$$

where $A_\xi=\begin{bmatrix}\bar{A} & -L\\ \bar{C}^T\bar{C} & \bar{A}^T-Q\end{bmatrix}\in\mathbb{R}^{(2n+2)\times(2n+2)}$.

B. Generic Conditions

The fact that the proposed ESO partially jumps when a new measurement arrives indicates that the updating process of the error dynamics can be classified as a sampled-data system. Such a system can be regarded as a combination of a continuous time system (18) and a reset integral operator (17). In view of this, in this subsection we consider the following general nonlinear sampled-data system:

$$\begin{cases}\dot{\xi}(t)=f_\xi(t,\xi(t),d(t),\rho(t)),\ \forall t\in[t_0,\ \infty)\\ \rho(t)=\Omega_\xi(\xi(t)),\ \forall t\in[t_k,\ t_{k+1}),\ k\in\mathbb{N}.\end{cases}\tag{19}$$

Here $f_\xi(t,\xi(t),d(t),\rho(t))\in C([t_0,\ \infty]\times\mathbb{R}^{m+m_p+1},\ \mathbb{R})$ is a continuous nonlinear function, $\xi(t)\in\mathbb{R}^m$ is the state vector, $d(t)\in\mathbb{R}^{m_p}$ represents some bounded perturbations such as external disturbances and unknown nonlinearities, $\Omega_\xi(\cdot)$ is a reset operator in the following form:

$$\Omega_\xi:\begin{cases}\rho(t)=\displaystyle\int_{t_k}^{t}\varphi_\xi(\xi(s))ds,\ \ \forall t\neq t_k\\ \rho(t_k)=0\end{cases}\tag{20}$$

with a continuous function $\varphi_\xi(\cdot)\in C(\mathbb{R}^m,\ \mathbb{R})$. Worthy of mention is that system (19)–(20) represents a large range of nonlinear sampled data systems discussed in related literature. See for instance the works of [26] and [28]. The error dynamics of the ESO in Section IV. A is a special case of (19)–(20). Therefore, we present generic conditions for the exponentially input-to-state stable (eISS) properties of system (19)–(20) with respect to $d(t)$.

Definition 1: Consider the sampled-data system (19)–(20). Regard $d(t)$ as the input of the system. For each $(t_0,\ \xi_0)\in\mathbb{R}^+\times\mathbb{R}^m$ and $\|d(t)\|\leq\bar{d}$. If there exists a continuous function $\xi(t,t_0,\xi_0)$ with the initial state $\xi(t_0)=\xi_0$ satisfying (19) for all $t\geq t_0$, then $\xi(t,t_0,\xi_0)$ is called a solution of the system (19). What is more, the system (19) is said to be exponentially input-to-state stable if there exist a unique solution $\xi(t,t_0,\xi_0)$ and three positive constants a, b, and c, independent of ξ_0, such that

$$\|\xi(t,t_0,\xi_0)\|\leq ae^{-b(t-t_0)}\|\xi_0\|+c\bar{d},\ \ \forall t\geq t_0.\tag{21}$$

The criteria for determining whether a system is eISS can be summarized as the following theorem.

Theorem 1: Consider the system (19)–(20) subject to Assumption 3. For any initial state $\xi(t_0)$, if system (19)–(20) admits a unique solution and there exist a differentiable, positive definite function $v(\xi(t))\in C(\mathbb{R}^m,\ \mathbb{R}^+)$, and constants $\alpha_2,\ \beta_2,\ \gamma,\ c_{21},\ c_{22}>0,\ r\geq 1,\ \theta=1/r$ such that for any $\xi(t)\in\mathbb{R}^m$

$$\alpha_2-\beta_2\tau_M>0\tag{22}$$

$$c_{21}\|\xi(t)\|^r\leq v(\xi(t))\leq c_{22}\|\xi(t)\|^r\tag{23}$$

$$\dot{v}(\xi(t))+\alpha_2 v(\xi(t))\leq\beta_2 v^{1-\theta}(\xi(t))\int_{t_k}^{t}v^\theta(\xi(s))ds+\gamma\|d(t)\|v^{1-\theta}(\xi(t))\tag{24}$$

hold for all $t\in[t_k,\ t_{k+1})$, $k\in\mathbb{N}$. Then for any $\xi_0\in\mathbb{R}^m$, the system is eISS with respect to $d(t)$, namely

$$\|\xi(t)\|\leq\frac{c_{22}^\theta}{c_{21}^\theta}e^{-\mu(t-t_0)}\|\xi(t_0)\|+\frac{\gamma\bar{d}\tau_M}{c_{21}^\theta}\left(1+\frac{1}{1-e^{-\mu\tau_m}}\right)\quad\forall t\geq t_0\tag{25}$$

where

$$\mu=(\alpha_2-\beta_2\tau_M)\theta e^{-\alpha_2\theta\tau_M}\tag{26}$$

is the exponential decay rate.

Proof: Let $v_1(\xi(t))=v^\theta(\xi(t))$. Using the result of Lemma 2.1 in [25], we obtain

$$v_1(\xi(t))\leq e^{-\mu(t-t_0)}v_1(\xi(t_0))+\gamma\bar{d}\tau_M\left(1+\frac{1}{1-e^{-\mu\tau_m}}\right).$$

Recall that (23) holds for all $t\geq t_0$, then it yields

$$(c_{21}\|\xi(t)\|^r)^\theta\leq v_1(\xi(t))\leq e^{-\mu(t-t_0)}(c_{22}\|\xi(t_0)\|^r)^\theta+\gamma\bar{d}\tau_M\left(1+\frac{1}{1-e^{-\mu\tau_m}}\right).$$

Note that $r\theta=1$, the above inequality is further simplified as

$$\|\xi(t)\|\leq\frac{c_{22}^\theta}{c_{21}^\theta}e^{-\mu(t-t_0)}\|\xi(t_0)\|+\frac{\gamma\bar{d}\tau_M}{c_{21}^\theta}\left(1+\frac{1}{1-e^{-\mu\tau_m}}\right).$$

■

The integral item $\beta_2 v^{1-\theta}(\xi(t))\int_{t_k}^{t}v^\theta(\xi(s))ds$ in (24) can be viewed as a storage term which guarantees the exponential dissipativeness of system (19)−(20) in the consideration of the sampling. The works in [28] and [43] replace this term by exploring a so-called storage function and finally obtain tractable stability criteria in terms of linear matrix inequalities. In this paper, we formulate the eISS condition based on the existence of a Lyapunov function, which is the extension of Lemma 2.1 in [25].

C. Main Results of the ESO

Base on the eISS analysis for the more general sample-data system (19)–(20), we obtain the main results about the estimation capability of the proposed ESO by embedding (17)–(18) into (19)–(20).

Come back to the condensed error dynamics of the ESO in (17)–(18), the item $h(t)$ can be specified as

Authorized licensed use limited to: TU Delft Library. Downloaded on February 02,2023 at 10:39:32 UTC from IEEE Xplore. Restrictions apply.

$$
\begin{aligned}
h &= \dot{f}(t,x,z,\omega) + \dot{g}_\Delta(t,x,z,\omega)u(t) + g_\Delta(t,x,z,\omega)\dot{u}(t) \\
&= \frac{\partial f(\cdot)}{\partial t} + \sum_{i=1}^{n-1}\frac{\partial f(\cdot)}{\partial x_i}x_{i+1}(t) + \frac{\partial f(\cdot)}{\partial x_n} \\
&\quad \times (f(t,x,z,\omega) + g_\Delta(t,x,z,\omega)u(t)) \\
&\quad + f_0(t,x,z,\omega)\frac{\partial f(\cdot)}{\partial z} + \dot{\omega}\frac{\partial f(\cdot)}{\partial \omega} \\
&\quad + (\dot{g}(t,x,z,\omega) - \dot{g}_0(x))Mg_\varepsilon\left(\frac{u_0\left(\bar{\hat{x}}_n\right) - \hat{x}_{n+1}}{g_0\left(\bar{\hat{x}}_n\right)M}\right) \\
&\quad + (g(t,x,z,\omega) - g_0(x))\frac{dg_\varepsilon(r)}{dr} \\
&\quad \times \frac{\left(\dot{u}_0\left(\bar{\hat{x}}_n\right) - \dot{\hat{x}}_{n+1}\right)g_0\left(\bar{\hat{x}}_n\right) - \left(u_0\left(\bar{\hat{x}}_n\right) - \hat{x}_{n+1}\right)\dot{g}_0\left(\bar{\hat{x}}_n\right)}{g_0^2\left(\bar{\hat{x}}_n\right)}.
\end{aligned}
$$

By Assumptions 1 and 2, if $x(t)$ is bounded, ω, $f_0(\cdot)$, $f(\cdot)$, and their partial derivatives are all bounded. Additionally, it follows from (9) and (10) that $|u(t)| \le M(1+\varepsilon/2)$ and $|\frac{dg_\varepsilon(r)}{dr}| \le 1$ for all $t \ge t_0$. Therefore, considering Assumptions 1, 2, and 6, we have that there exist two ε-independent positive constants N_1, N_2, such that the differentiation of the perturbed item in (18) is bounded in the sense of

$$
\|\bar{D}h(t) + \bar{B}g_\Delta u(t)\| \le N_1 + N_2\|\eta\|, \quad \forall t \ge t_0. \tag{27}
$$

If L and Q are selected so that $A_\xi = \begin{bmatrix} \bar{A} & -L \\ \bar{C}^T\bar{C} & \bar{A}^T - Q \end{bmatrix}$ is Hurwitz, there exist a symmetric positive definite matrix $P > 0$ and a positive constant κ such that

$$
A_\xi^T P + PA_\xi \le -2\kappa I_{2n+2}. \tag{28}
$$

The following theorem generalizes the stability analysis results of the proposed ESO.

Theorem 2: Consider the system (1) which is observed by the ESO (5)–(7). Suppose that Assumptions 1–3, 5, and 6 hold and the state $x(t)$ is bounded by $x(t) \in \mathcal{X}$, $\forall t \ge t_0$, where $\mathcal{X}$ is a compact set. Denote $\varepsilon^* = \frac{\kappa - \kappa_1\lambda_{P,\max}}{N_2\ell_P\lambda_{P,\max}}$ and $\delta_M = \kappa_1/(2\sqrt{\ell_P})$, where $\kappa_1 \in (0, \kappa/\lambda_{P,\max})$

1) If $\tau_M < \varepsilon^*\delta_M$, then for any $\varepsilon \in (\tau_M/\delta_M\ \varepsilon^*)$, the solution of the error dynamics (17) and (18) is eISS with respect to the unknown nonlinearity $\bar{D}h(t) + \bar{B}g_\Delta u(t)$.

2) Furthermore, if $\tau_M < \varepsilon^*\delta_M$, then for any $\varepsilon \in (\tau_M/\delta_M, \varepsilon^*)$, $\sup_{t\in[t_0+T(\varepsilon),\,\infty)}\|\xi(t)\| = O(\varepsilon)$. where $T(\varepsilon) > 0$ and $T(\varepsilon) \to 0$ as $\varepsilon \to 0$.

Proof: Consider the Lyapunov function candidate $V_2(\xi(t)) = \xi^T(t)P\xi(t)$ and differentiate it along (18)

$$
\begin{aligned}
\dot{V}_2(\xi(t)) &\le -\frac{2\kappa}{\varepsilon}\|\xi(t)\|^2 + 2\xi^T(t)P\begin{pmatrix} \bar{D}h(t) + \bar{B}g_\Delta u(t) \\ \bar{C}^T\frac{\rho(t)}{\varepsilon} \end{pmatrix} \\
&\le -\frac{2\kappa}{\varepsilon}\|\xi(t)\|^2 + 2\left\|\xi^T(t)P\right\| \\
&\quad \times\left(\|\bar{D}h(t) + \bar{B}g_\Delta u(t)\| + \frac{1}{\varepsilon^2}\int_{t_k}^t |\eta_2(s)|ds\right).
\end{aligned} \tag{29}
$$

In view of (27), $\lambda_{P,\min}\|\xi(t)\|^2 \le V_2(\xi(t)) \le \lambda_{P,\max}\|\xi(t)\|^2$ and $\left\|\xi^T(t)P\right\| \le \sqrt{\lambda_{P,\max}V_2(\xi(t))}$, (29) can be released as

$$
\begin{aligned}
\dot{V}_2(\xi(t)) &\le -\frac{2\kappa}{\varepsilon\lambda_{P,\max}}V_2(\xi(t)) + 2\lambda_{P,\max}\|\xi(t)\| \\
&\quad \times\left(N_1 + N_2\|\eta\| + \frac{1}{\varepsilon^2}\int_{t_k}^t\|\xi(s)\|ds\right) \\
&\le -\left(\frac{2\kappa}{\varepsilon\lambda_{P,\max}} - 2N_2\ell_P\right)V_2(\xi(t)) \\
&\quad + 2N_1\sqrt{\lambda_{P,\max}}\sqrt{V_2(\xi(t))} \\
&\quad + \frac{2\sqrt{\ell_P}}{\varepsilon^2}\sqrt{V_2(\xi(t))}\int_{t_k}^t\sqrt{V_2(\xi(s))}ds.
\end{aligned} \tag{30}
$$

By comparing the right side of (30) and (24), we can find that if we choose $\varepsilon^* = \frac{\kappa - \kappa_1\lambda_{P,\max}}{N_2\ell_P\lambda_{P,\max}}$, for any $\varepsilon \in (0, \varepsilon^*)$, we have $\frac{2\kappa}{\varepsilon\lambda_{P,\max}} - 2N_2\ell_P > 2\kappa_1/\varepsilon$. Then, $V_2(\xi(t))$ just satisfies (24) with

$$
r = 2,\ \theta = \frac{1}{2},\ \alpha_2 = \frac{2\kappa_1}{\varepsilon},\ \beta_2 = \frac{2\sqrt{\ell_P}}{\varepsilon^2}
$$

$$
\gamma = 2N_1\sqrt{\lambda_{P,\max}},\ c_{21} = \lambda_{P,\min},\ c_{22} = \lambda_{P,\max}.
$$

Thus, taking $\delta_M = \kappa_1/(2\sqrt{\ell_P})$ we can find that for all $\tau_M \le \delta_M\varepsilon$, we have

$$
\alpha_2 - \beta_2\tau_M \ge \frac{\kappa_1}{\varepsilon} > 0. \tag{31}
$$

The combination of (30) and (31) shows that the Lyapunov function candidate $V_2(\xi(t))$ falls in the class of functions $v(\xi(t))$ presented in Theorem 1. Recall that the error dynamics (17)–(18) is a kind of system described in Section IV-B. Therefore, according to Theorem 1, the solution of (18) satisfies the following inequality:

$$
\begin{aligned}
\|\xi(t)\| &\le \sqrt{\ell_P}e^{-\mu(t-t_0)}\|\xi(t_0)\| \\
&\quad + 2\sqrt{\ell_P}\tau_M N_1\left(1 + \frac{1}{1 - e^{-\mu\tau_m}}\right)
\end{aligned} \tag{32}
$$

where the decay rate μ is equal to $(\kappa_1/\varepsilon - \sqrt{\ell_P}\tau_M/\varepsilon^2)e^{-\kappa_1\tau_M/\varepsilon}$. This proves the first proposition of Theorem 2.

Furthermore, since $\tau_M \le \kappa_1\varepsilon/(2\sqrt{\ell_P})$, and $\mu(\tau_M) = (\kappa_1/\varepsilon - \sqrt{\ell_P}\tau_M/\varepsilon^2)e^{-\kappa_1\tau_M/\varepsilon}$ is a strictly decreasing function with respect to τ_M, we obtain

$$
\mu = \mu(\tau_M) \ge \mu(\varepsilon\delta_M) = \frac{\kappa_1}{2\varepsilon}e^{-\frac{\kappa_1^2}{2\sqrt{\ell_P}}} = \frac{N_3}{\varepsilon} \tag{33}
$$

where $N_3 = \frac{\kappa_1}{2}e^{-\kappa_1^2/(2\sqrt{\ell_P})}$ is a constant independent of ε. After taking into account (32) and (33) we can get that $\|\xi(t)\|$ satisfies

$$
\begin{aligned}
\|\xi(t)\| &\le \sqrt{\ell_P}e^{-\frac{N_3(t-t_0)}{\varepsilon}}\|\xi(t_0)\| \\
&\quad + \sqrt{\ell_P}\delta_M N_1\left(1 + \frac{1}{1 - e^{-\frac{N_3\tau_m}{\varepsilon}}}\right)\varepsilon.
\end{aligned} \tag{34}
$$

The right side of (34) tends to zero as $\varepsilon \to 0$. More specifically, by taking $T(\varepsilon) = -\varepsilon\ln\varepsilon$, we can see that there exists an ε^* such that if $\tau_M < \varepsilon^*\delta_M$, then for any $\varepsilon \in (\tau_M/\delta_M, \varepsilon^*)$, $\sup_{t\in[t_0+T(\varepsilon),\,\infty)}\|\xi(t)\| = O(\varepsilon)$ holds. ■

Authorized licensed use limited to: TU Delft Library. Downloaded on February 02,2023 at 10:39:32 UTC from IEEE Xplore. Restrictions apply.

D. Checking Assumption 5

From the proving progress of Theorem 2, one can observe that the existence of the Lyapunov function $V_2(\xi(t))$ principally depends on whether the matrix A_ξ is Hurwitz. In the following we will demonstrate that by selecting l_i and q_i, $i = 1, 2, \ldots, n+1$ one can assign the eigenvalues of A_ξ to make Assumption 5 satisfied.

Let $\lambda \in \mathbb{C}$ be an arbitrary complex number. Define a set of matrices

$$G_{2j} = \begin{pmatrix} -\lambda I_j + A_j & -L_j \\ C_j^T C_j & -\lambda I_j + A_j^T - Q_j \end{pmatrix}, \quad j = 1, \ldots, n+1$$

where A_j, L_j and Q_j are the j th sequential principal minor matrices of $\bar{A}$, L, and Q, respectively, and $C_j = [1, 0, \ldots, 0] \in \mathbb{R}^{j\times 1}$. From the definition of G_{2j} we can readily know that $G_{2n+2} = A_\xi - \lambda I_{2n+2}$. Next, we will iteratively show that one can select appropriate $l_1, l_2, \ldots, l_j$ and $q_1, q_2, \ldots, q_j$ to assign the roots of the equation $\det(G_{2j}) = 0$ arbitrarily and thus make A_ξ Hurwitz. The design procedure is similar to that in [29], while the difference is that we use Laplace expansion to simplify the design.

Step 1: Let $j = 1$, then $G_{2j} = \begin{pmatrix} -\lambda & -l_1 \\ 1 & -\lambda - q_1 \end{pmatrix}$. The determinant of G_2 is $\lambda^2 + q_1\lambda + l_1$. It is obviously simple to make $\det(G_2)$ be a Hurwitz polynomial. Namely, if the target Hurwitz polynomial is $P_2(\lambda) = \lambda^2 + a_1\lambda + a_2$, one can directly choose $q_1 = a_1$, $l_1 = a_2$ to make $\det(G_2) = P_2(\lambda)$.

Step 2: When $j > 1$, let us first detect the relationship between $\det(G_{2j})$ and $\det(G_{2j-2})$. By using the Laplace expansion theorem, we expand the determinant of G_{2j} along the jth and $2j$th lines of G_{2j}, we obtain

$$\det\left(G_{2j}\right) = \lambda\left(\lambda + q_j\right)\det\left(G_{2j-2}\right) + l_i. \tag{35}$$

Let $P_{2j}(\lambda) = \lambda^{2j} + \sum_{s=1}^{2j} a_s^{(j)}\lambda^{2j-s}$ be an arbitrary target Hurwitz polynomial, then it can be rewritten as

$$\begin{aligned} P_{2j}(\lambda) &= \lambda\left(\lambda^{2j-1} + \sum_{s=1}^{2j-1} a_s^{(j)}\lambda^{2j-1-s}\right) + a_{2j}^{(j)} \\ &= \lambda R_j(\lambda) + a_{2j}^{(j)} \end{aligned} \tag{36}$$

where $R_j(\lambda) = \lambda^{2j-1} + \sum_{s=1}^{2j-1} a_s^{(j)}\lambda^{2j-1-s}$. We take into consideration that $R_j(\lambda)$ is an odd-order Hurwitz polynomial, so there must exist at least one real negative root which denoted by $-\lambda_j$. Then, the target polynomial for $\det(G_{2j-2})$ is designed as

$$P_{2j-2}(\lambda) = \frac{R_j(\lambda)}{\lambda + \lambda_j}. \tag{37}$$

Combined with (37), (36) yields

$$P_{2j}(\lambda) = \lambda\left(\lambda + \lambda_j\right)P_{2j-2}(\lambda) + a_{2j}^{(2j)}. \tag{38}$$

Comparing the right side of (35) and (38), we can see that by choosing $q_j = \lambda_j$, $l_j = a_{2j}^{(j)}$, we can guarantee that the determinant of G_{2j} matches the Hurwitz polynomial $P_{2j}(\lambda)$. Furthermore, by iteratively using the above method for $j = n+1, n, \ldots, 2, 1$, we can complete the design task of L and Q and finally construct a Hurwitz matrix A_ξ.

The above two steps indicate a feasible design procedure of l_i and q_i, $i = 1, 2, \ldots, n+1$, which can be summarized as follows.

Step 1: Initialize a target Hurwitz polynomial $P_{2n+2}(\lambda) = \lambda^{2n+2} + \sum_{s=1}^{2n+2} a_s^{(n+1)}\lambda^{2n+2-s}$ and let $j = n+1$.

Step 2: i) For given $P_{2j}(\lambda) = \lambda^{2j} + \sum_{s=1}^{2j} a_s^{(j)}\lambda^{2j-s}$, choose $l_j = a_{2j}^{(j)}$.

ii) Search one real negative root (denoted by $-\lambda_j$) of the polynomial $R_j(\lambda) = \lambda^{2j-1} + \sum_{s=1}^{2j-1} a_s^{(j)}\lambda^{2j-1-s}$ and let $q_j = \lambda_j$.

iii) If $j \geq 2$, determine the next polynomial $P_{2j-2}(\lambda)$ to $\frac{R_j(\lambda)}{\lambda+\lambda_j}$ and let $j \to j-1$. Then go back to Step 1. If $j = 1$, the design procedure is finished.

V. Closed-Loop Performance

The previous section indicates that under the condition that the state trajectory of the system is bounded, the estimation error of the ESO is convergent. Based on Theorem 2, in the following lemma we will show the boundedness of the closed-loop system's trajectory under the ADRC law (5)−(9) in Lemma 1, where the condition $x(t) \in \mathcal{X}$, $t \geq t_0$ involved in the previous section will be removed. Based on Lemma 1 and Theorem 1, we are in the position to state our main result in Theorem 3, which concludes the convergence level and rate for the closed-loop system.

Let $\varsigma_1 = \sup_{\|x(t)\| \leq \|x(t_0)\|} V_1(x(t)) + 1$, where $V_1(x(t))$ is a function satisfying Assumption 4. Then, let us first define two compact sets as below

$$\begin{cases} \Xi_1 = \{x(t) \in \mathbb{R}^n : \ V_1(x(t)) \leq \varsigma_1\} \\ \Xi_2 = \{x(t) \in \mathbb{R}^n : \ V_1(x(t)) \leq \varsigma_2\} \end{cases} \tag{39}$$

where $\varsigma_2 \in (\varsigma_1, \infty)$. From (39), it can be readily detected that $x(t_0) \in \Xi_1$ and $\Xi_1 \subset \Xi_2$. The following lemma will show that under some conditions, $x(t)$ starting in Ξ_1 will always stay in Ξ_2.

Lemma 1: Consider the closed-loop system consisting of (1), the ESO (5)–(7) and the controller (8)–(9). Suppose Assumptions 1–6 are satisfied. Denote $\delta_M = \kappa_1/(2\sqrt{\ell_P})$, where $\kappa_1 \in (0, \kappa/\lambda_{P,\max})$. There exists an ε_1 such that if $\tau_M < \varepsilon_1\delta_M$, then $\forall \varepsilon \in (\tau_M/\delta_M, \varepsilon_1)$ and $\forall t \geq t_0$, $x(t) \in \Xi_2$ holds.

Proof: Remark that $x(t_0)$ is an interior point of Ξ_1 and the solution $x(t)$ is continuous in the time interval $[t_0, \infty)$. Therefore, there must exist a point of time $t_a > t_0$ such that $x(t) \in \Xi_1$ holds for all $t \in [t_0, t_a]$. Next, we will use contradiction to complete the rest of the proof. Assume that Lemma 1 is not true, then according to the continuity of $x(t)$, there exists a period of time when the trajectory $x(t)$ escapes from Ξ_1 and reaches the boundary of Ξ_2. That is to say, $\exists t_c > t_b > t_a$ such that

$$\begin{cases} V_1(x(t_b)) = \varsigma_1 \\ V_1(x(t_c)) = \varsigma_2 \\ \varsigma_1 \leq V_1(x(t)) \leq \varsigma_2, \ t \in [t_b, t_c] \\ V_1(x(t)) \leq \varsigma_2, \ \ t \in [t_0, t_c]. \end{cases} \tag{40}$$

Authorized licensed use limited to: TU Delft Library. Downloaded on February 02,2023 at 10:39:32 UTC from IEEE Xplore. Restrictions apply.

Then for any $t \in [t_0, t_c]$, $\sqrt{\varsigma_2/c_{12}} \le \|x(t)\| \le \sqrt{\varsigma_2/c_{11}}$ and hence all the conditions in Theorem 2 are satisfied. Therefore, we can conclude that for $\forall \varepsilon \in (\tau_M/\delta_M, \varepsilon^*)$, (34) holds in the time interval $[t_0, t_c]$. Additionally, from (10) we observe that $\hat{x}_i(t) \le |x_i(t)| + \varepsilon^{n+1-i}|\eta_i(t)|$, $i = 1, \ldots, n+1$, so we can choose $M > \sup_{t\in[t_0,\, t_c]} |(u_0(x(t)) - x_{n+1}(t))/g(x(t))|$ such that the control input (9) is never saturated during the time interval $[t_0, t_c]$. Based on Assumption 4, calculating the time derivative of $V_1(x(t))$ alone (1), we deduce

$$\begin{aligned}
\dot{V}_1(x(t)) &= \sum_{i=1}^{n-1} x_{i+1}(t) \frac{\partial V_1(x(t))}{\partial x_i(t)} \\
&\quad + \left(x_{n+1} + u_0\left(\bar{\hat{x}}_n\right) - \hat{x}_{n+1}\right) \frac{\partial V_1(x(t))}{\partial x_n(t)} \\
&= \sum_{i=1}^{n-1} x_{i+1}(t) \frac{\partial V_1(x(t))}{\partial x_i(t)} + u_0(x) \frac{\partial V_1(x(t))}{\partial x_n(t)} \\
&\quad + \left(\eta_{n+1} + u_0\left(\bar{\hat{x}}_n\right) - u_0(x)\right) \frac{\partial V_1(x(t))}{\partial x_n(t)} \\
&\le -\alpha_1 V_1(x(t)) + N_4\beta_1 \|\eta(t)\| \|x(t)\| \\
&\le -\alpha_1 c_{11} \|x(t)\| \left(\|x(t)\| - \frac{N_4\beta_1}{\alpha_1 c_{11}} \|\eta(t)\|\right) \qquad (41)
\end{aligned}$$

where N_4 is an ε-independent positive constant. Recall that $\xi(t)$ is an extended vector of $\eta(t)$ and satisfies (34), so we can select ε to be enough small such that $\|\eta(t)\| \le \|\xi(t)\| \le \frac{\alpha_1 c_{11}}{N_4\beta_1} \sqrt{\varsigma_2/c_{12}}$, $\forall t \in [t_0, t_c]$. In other words, there exists an $\varepsilon_1 \in (0, \varepsilon^*)$ such that if $\tau_M < \varepsilon_1 \delta_M$ is satisfied, then

$$\dot{V}_1(x(t)) < 0 \qquad (42)$$

holds for any $\varepsilon \in (\tau_M/\delta_M, \varepsilon_1)$ and $t \in [t_b, t_c]$. The inequality (42) contradicts (40). ■

Finally, we are ready to present our main results on the proposed ADRC structure.

Theorem 3: Consider the closed-loop system composed of (1) and (5)–(9). Suppose that Assumptions 1–5 are satisfied. Denote $\delta_M = \kappa_1/(2\sqrt{\ell_P})$, where $\kappa_1 \in (0, \kappa/\lambda_{P,\max})$. For any $x(t_0) \in \Xi_1$, there exists an ε_1 such that if $\tau_M < \varepsilon_1 \delta_M$, then $\forall \varepsilon \in (\tau_M/\delta_M, \varepsilon_1)$ and $\forall t \ge t_0$,

$$\sup_{t\in[t_0+T(\varepsilon),\, \infty)} \|\xi(t)\| = O(\varepsilon) \qquad (43)$$

$$\sup_{t\in[t_0+T(\varepsilon),\, \infty)} |x_i(t) - \hat{x}_i(t)| = O(\varepsilon^{n+2-i}),\ i = 1, \ldots, n+1 \qquad (44)$$

$$\lim_{t\to\infty} \|x(t)\| = O(\varepsilon) \qquad (45)$$

where $T(\varepsilon) > 0$ and $T(\varepsilon) \to 0$ as $\varepsilon \to 0$.

Proof: In the proving procedure of Lemma 1, we have derived that the trajectory of the closed-loop system starting in Ξ_1 will be bounded by $x(t) \in \Xi_2$, $\forall t \in [t_0, \infty)$. This yields that (34) holds for all $t \in [t_0, \infty)$. By taking $T(\varepsilon) = -\varepsilon \ln \varepsilon > 0$ we can derive (43). Note that $x_i(t) - \hat{x}_i(t) = \varepsilon^{n+1-i}\eta_i(t)$ and $\xi^T(t) = [\eta^T(t), \chi^T(t)]$, then we get (44). Moreover, note that (41) holds uniformly in $t \in [t_0, \infty)$, by using $\frac{d\sqrt{V_1(x(t))}}{dt} = \frac{1}{2\sqrt{V_1(x(t))}} \frac{dV_1(x(t))}{dt}$, the following relationship is derived:

$$\frac{d\sqrt{V_1(x(t))}}{dt} \le -\frac{\alpha}{2}\sqrt{V_1(x(t))} + \frac{N_5\varepsilon}{2} \qquad (46)$$

where N_5 is an ε-independent positive constant. From (46) and the fact that $c_{11}\|x(t)\|^2 \le V_1(x(t))$, we can deduce (45). ■

Remark 3: We should point out that some other output feedback methods, such as continuous-discrete time high gain observer [25] based high gain control [44] can likewise be a valuable tool to make the system's trajectory as small as expected under additional conditions like the nonlinearity $f(\cdot)$ being Lipachitz continuous. However, when the value of $f(t, x, z, \omega)$ is large, both the gains of the observer and the controller have to be large enough to accommodate large uncertainty. The observer and controller with such large gains are a waste of energy in practical application and may make the resulting system peak during the transient period [45], [46]. In this paper, although a moderately large gain in the proposed ESO is still necessary, the gain in the control law $u_0(\cdot)$ is not required to be large thanks to the cancellation of uncertainty, and the peaking phenomena will be restrained by introducing the saturation function. This fact will be verified in Section VI.

Remark 4: It is worthy to notice that the calibration of the proposed continuous time ESO is chiefly dependent on the adjustment of the gain parameter ε. From Theorem 3, one can find that for the concerned system with sampled measurements, the lower bound of ε is limited by the maximum sampling interval. This characteristic is similar to that of ADRC design for time-delay systems in [13]. The explanation of this coincidence lies in the fact that both the ADRC schemes in this paper and in [13] contain state predictors whose predictive capability is constrained by the maximum sampling interval, or maximum delay. On the other hand, it is worthwhile to mention here that in most results on the traditional ADRC design [10]–[12], the value of ε can be tuned to be arbitrarily small to obtain better estimation capacity and faster convergence rate. In this respect, combined with the results in [13], the results in this paper can provide a general guideline for the predictor-based ADRC design.

Remark 5: When the system is attached with measurement noise, it has been reported in [47] that there exists a tradeoff between the error due to system uncertainty and the error due to sensor noise. Meanwhile, experiments have shown that too small ε causes high-frequency oscillations in control signal because of amplification of measurement noise [39]. Therefore, there are some practical limitations on the value of ε when the control algorithm is implemented. To alleviate the negative effect of measurement noise, one can employ the idea of switched-gain [47], which can realize a better balance between system uncertainty and sensor noise. This issue deserves detailed investigation in the future.

Remark 6: For (1), additive disturbances can be added to $f(\cdot)$ and $g(\cdot)$, regarded as the "total uncertainty" in ADRC structure. As a result, as long as the new $f(\cdot)$ and $g(\cdot)$ satisfy Assumptions 1 and 6, the proposed ADRC is still a reliable

Authorized licensed use limited to: TU Delft Library. Downloaded on February 02,2023 at 10:39:32 UTC from IEEE Xplore. Restrictions apply.

scheme. It should also be emphasized that the results of the proposed ADRC scheme can be extended to systems with input uncertainty, or even mismatched uncertainty. To deal with the input uncertainty, one can readily adopt the method in [12], where a projection gradient estimator is constructed to separate input uncertainty from total uncertainty. To accomplish mismatched one, the coordinate transformation [11] can be an appropriate approach to convert systems with mismatched uncertainty into the form of (1).

Remark 7: There are several groups of parameters that need to be determined in our presented ESO-based disturbance rejection scheme.

1) For the predictor-based ESO (5)–(7), the parameters to be designed are the gains l_i, q_i, and ε, $i=1,\ldots,n+1$. The selection of l_i and q_i can be iteratively completed via the pole placement algorithm in Section IV-D, so that the matrix A_ξ becomes Hurwitz. The value of ε is supposed to be small to attain more accurate estimation. However, the minimum acceptable value of ε is prescribed by the maximum sampling interval. As for implementation, the value of ε can be assigned by some trial and error experiments, based on the recovery performance of the system.

2) For the control device (8)–(11), the parameters include the feedback gains k_i and the saturation bound M for u_{nom}. The values of k_i can be set through various methods commonly used in feedback control of linear systems, such as pole placement technique and linear quadratic regulator. The value of M is usually decided according to the physical or geometric constraints of the actual actuator. From a theoretical point of view, the saturation bound should be selected such that the saturation will not be invoked under state feedback [34], that is $M > \sup|u_0(x(t)) - x_{n+1}(t)/g(x(t))|$.

VI. Numerical Simulations

In this section, two examples are given to show the performance of the proposed control scheme.

A. Example 1

Consider the following uncertain nonlinear system with sampled measurements:

$$\begin{cases} z(t) = -\left(x_1^2(t)+1\right)z(t) \\ x_1(t) = x_2(t) \\ x_2(t) = f(t,x(t),z(t),\omega(t)) + g(t,x(t),z(t),\omega(t))u(t) \\ \omega(t) = \dfrac{\sin(2t)}{2} \\ y(t_k) = x_1(t_k),\ t \geq t_0,\ k \in \mathbb{N} \end{cases} \tag{47}$$

where $f(t,x(t),z(t),\omega(t)) = \sin(x_1(t)) + x_1(t)x_2^2(t) + \sin(t) + z(t)x_1(t) + \omega(t)x_2(t) + \omega(t)$, $g(t,x(t),z(t),\omega(t)) = 1 + g_\Delta(t,x(t),z(t),\omega(t))$ with the unknown part $g_\Delta(\cdot) = 0.5 + 0.2\sin(x_1(t))$, and t_k is the sampling time with the interval

$$\tau_k = t_{k+1} - t_k = \begin{cases} 0.1, & \text{if } k \text{ is odd} \\ 0.05, & \text{else.} \end{cases}$$

It is apparent that $f(\cdot)$, $g(\cdot)$, $\omega(t)$ and τ_k satisfy Assumptions 1, 3, and 6, and Assumption 2 can be effortlessly verified by considering the Lyapunov candidate $V_0(z) = z^2(t)/2$. From (47), we have $\frac{\partial V_0}{\partial z}(z) f_0(\cdot) = -(x_1^2(t)+1)z^2(t) \leq 0$. Therefore, the proposed ADRC can be applied.

For the design of the ESO, take $x_3 = f(\cdot) + g_\Delta(\cdot)u$ as the extended state. The coefficients of the gain matrices L and Q are iteratively computed such that the matrix A_ξ defined in (18) has six identical eigenvalues located at -1. The algorithm detailed in the Section IV has been implemented to generate L and Q. The derived values are $L = \text{diag}\{3, 3, 1\}$ and $Q = \text{diag}\{2, 2, 2\}$. The value of ε is set to 0.05. The controller (8)–(9) is designed in a linear feedback form with $K = [-4, -4]$ and $M = 30$. Initial states of the plant (47) and the ESO (5)–(7) are fixed at $[x_1(0), x_2(0), z(0)]^T = [1, 1, 1]^T$ and $\hat{x}(0) = [0, 0, 0]^T$. The simulation results are depicted in Figs. 2 and 3, where one can observe that the ESO maintains satisfactory performance and the control input saturates at $\pm M$ during the peaking period.

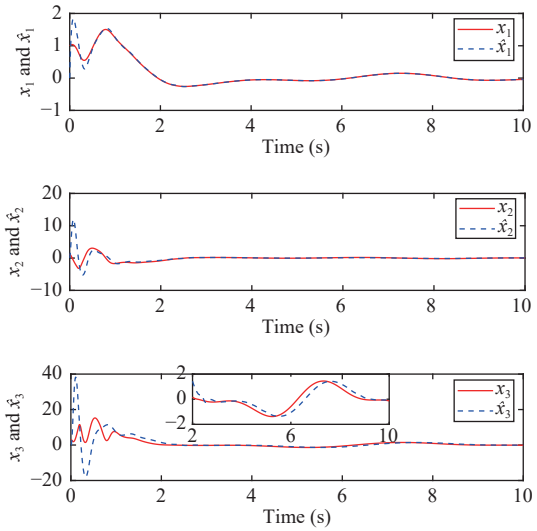

Fig. 2. System response and ESO output.

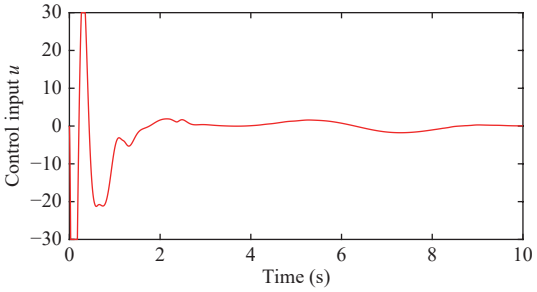

Fig. 3. Input signal u.

We further compare our new ADRC with the event-triggered ADRC established in [41]. The event-triggered ADRC develops a sample-data continuous ESO based on the fixed observation error $y(t_k) - \bar{C}\hat{x}(t_k)$. In order to highlight the comparison results, we set identical gains for both observers and controllers in our proposed scenario and the scenario in [41]. The simulation results are shown in Fig. 4 . As for different τ_k, we calculate the root mean squared errors (RMSE) of the system's state x and its estimation error $x - \hat{x}$

Authorized licensed use limited to: TU Delft Library. Downloaded on February 02,2023 at 10:39:32 UTC from IEEE Xplore. Restrictions apply.

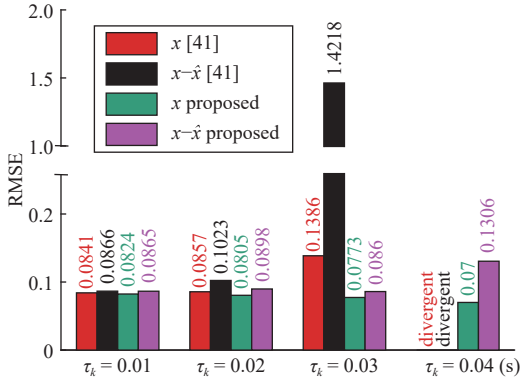

Fig. 4. The comparison of RMSE by using different approaches.

in the last eight seconds. It can be observed that when the sampling interval is small, both scenarios realize satisfactory control performance. However, the increase of τ_k results in much larger estimation error of the ESO in [41], or even divergence.

From a theoretical point of view, τ_M should satisfy $\tau_M < \varepsilon^* \delta_M$, given in Theorem 2. This condition seems to be pretty restrictive since it may result in the smaller allowable value of τ_M if ε is selected to be smaller. Nevertheless, this condition is conservatively prescribed, for the purpose of getting the convergence result of the ESO. Our simulation results in Fig. 4 have shown that the proposed scenario can perform effectively with sampling interval that are larger than the theoretical bound given in Theorem 2.

To further indicate the tradeoff between the error caused by model uncertainty and the error induced by measurement noise, we add a noise signal to the output of the system, that is $y(t_k) = x_1(t_k) + \Delta_m, t \geq t_0$, $k \in \mathbb{N}$, with $\Delta_m \in \mathbb{R}$ being the measurement noise. The magnitude of the noise is limited to 0.001. Table I summarizes the control performance under different parameter settings of ε.

TABLE I
RMSE OF THE SYSTEM'S STATE WITH MEASUREMENT NOISE

Values of ε	0.025	0.05	0.075	0.01
RMSE of x	0.461	0.152	0.133	0.141

As mentioned in Remark 7, the computation of the saturation bound M is not straightforward and one may end up with some conservative choices. In the first example, we further take different values for the saturation bound. Depicted in Fig. 5 , our numerical simulation indicates that a larger saturation bound is likely to contribute to a better transient performance.

B. Example 2

To further verify the applicability of the proposed approach, a simulation is carried out for a single-link flexible-joint robot manipulator [22], [48], whose dynamics can be expressed by the following equations:

$$\begin{cases} J_1 \ddot{q}_1 + f_1^* \dot{q}_1 + M^* g l^* \sin(q_1) + a^*(q_1 - q_2) = 0 \\ J_2 \ddot{q}_2 + f_2^* \dot{q}_2 - a^*(q_1 - q_2) = u \end{cases} \tag{48}$$

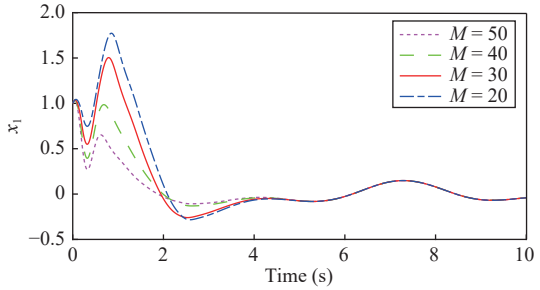

Fig. 5. System response under different saturation bounds.

where q_1 and q_2 denote the link angle and the motor angle, J_1 and J_2 stand for the link inertia and the motor inertia, respectively, M^* and l^* represent the mass and the length of the link, respectively, $g = 9.8\ \mathrm{m/s^2}$ is the gravitational acceleration, f_1^* and f_2^* is the friction coefficients of the link and the motor, respectively, and a^* is the joint stiffness. The control objective is to stabilize q_1 and q_2 at zero. Let $x_1 = q_1$, $x_2 = \dot{q}_1$, $x_3 = q_2$ and $x_4 = \dot{q}_2$, the dynamics (48) can be reformulated as the following first order differential equation form:

$$\begin{cases} \dot{x}_1 = x_2 \\ \dot{x}_2 = \dfrac{a^*}{J_1}(x_3 - x_1) - f_1^* x_2 - \dfrac{M^* g l^*}{J_1} \sin(x_1) \\ \dot{x}_3 = x_4 \\ \dot{x}_4 = \dfrac{a^*}{J_2}(x_1 - x_3) + \dfrac{1}{J_2}\left(u - f_2^* x_4\right). \end{cases} \tag{49}$$

We assume that only the link angle can be measured and the output is only available at sampling moments $t_k = \tau k$, $k \in \mathbb{N}$, where τ is the constant sampling interval. In this example, the values of the parameters in (49) are listed in Table II.

TABLE II
PARAMETERS OF THE ROBOT MANIPULATOR

Physical meaning	Symbol	Value
Link mass	M^*	1 kg
Link length	l^*	0.8 m
Link/motor inertia	J_1 and J_2	1 kg·m^2 and 1.2 kg·m^2
Joint stiffness	a^*	25 N
Link/motor friction coefficient	f_1^* and f_2^*	0.5 N·s and 1 N·s
Sampling intervals	τ	0.1 s

It should be noted that the exact values of the friction coefficients are not easy to obtain in practice, which makes the dynamics attached with mismatched uncertainty. As mentioned in Remark 6, combined with the coordinate transformation approach, the proposed ADRC scheme can be a feasible method to handle the issues considered. Namely, define new state variables $s = [s_1,\ s_2,\ s_3,\ s_4]^T$. Let $s_1 = x_1$, $s_2 = \dot{s}_1 = x_2$, $s_3 = \dot{s}_2 = \frac{a^*}{J_1}(x_3 - x_1) - f_1^* x_2 - \frac{M^* g l^*}{J_1} \sin(x_1) = b_3\left(x_1, x_2, x_3, f_1^*\right)$, $s_4 = \dot{s}_3 = \sum_{i=1}^{3} \frac{\partial b_3}{\partial x_i} \dot{x}_i = b_4\left(x, f_1^*, f_2^*\right)$, then we have

Authorized licensed use limited to: TU Delft Library. Downloaded on February 02,2023 at 10:39:32 UTC from IEEE Xplore. Restrictions apply.

$$\dot{s}_1 = s_2,\ \dot{s}_2 = s_3,\ \dot{s}_3 = s_4$$

$$\dot{s}_4 = \sum_{i=1}^{3} \frac{\partial b_4}{\partial x_i}\dot{x}_i + \frac{\partial b_4}{\partial x_4}\left(\frac{a^*}{J_2}(x_1 - x_3) + \frac{1}{J_2}\left(u - f_2^* x_4\right)\right)$$

$$= \bar{\phi}\left(s, f_1^*, f_2^*\right) + \frac{a^*}{J_1 J_2}u \tag{50}$$

where $\bar{\phi}(s, f_1^*, f_2^*)$ represents an unknown nonlinear function satisfying Assumption 1. By this formulation, the state stabilization of (49) can be achieved by the stabilization of s-system of (50) with the measured output $y(t_k) = s_1(t_k)$. The outputs of the ESO are accordingly the estimates of $s(t)$ and $\bar{\phi}t(s, f_1^*, f_2^*)$, instead of $x(t)$. The feedback controller is designed as (7) based on the continuous time ESO (5)–(7) with $L = \text{diag}\{5,\ 10,\ 10,\ 5,\ 1\}$, $Q = \text{diag}\{2,\ 2,\ 2,\ 2,\ 2\}$, $\varepsilon = 0.1$, $K = [-3,\ -5,\ -3,\ -1]$, $u_{\text{nom}}(t) = \frac{J_1 J_2}{a^*}(s_5(t) - 3s_1(t) - 5s_2(t) - 3s_3(t) - s_4(t))$ and $M = 8$. The initial conditions are taken as $x(0) = [-1,\ -1,\ -1.5,\ 1]^T$ and $\hat{s}(0) = [0,\ 0,\ 0,\ 0,\ 0]^T$.

The simulation results are plotted in Figs. 6 and 7. In Fig. 6, the convergence of the system state is shown and reverse calculation is used to obtain the estimate of $x(t)$ from $\hat{s}(t)$. It should be underlined that the purpose of this calculation is only to verify the results, while in practice, this calculation is not feasible because the friction coefficient cannot be determined. From Fig. 6, one can observe that obtained state estimates converge to the true value faster than the system state stabilizes to zero. This phenomenon indicates that the proposed ADRC possesses multi-time scale characteristics similarly to the general ADRC. What is more, to illustrate the robustness of the proposed method to small perturbations of sampling intervals, we show the change in the system response with different lengths of sampling intervals in Fig. 8.

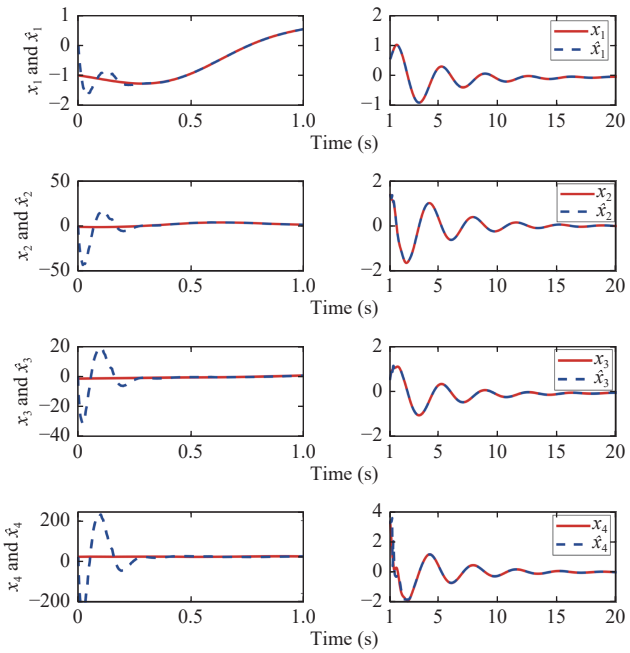

Fig. 6. System response and ESO output.

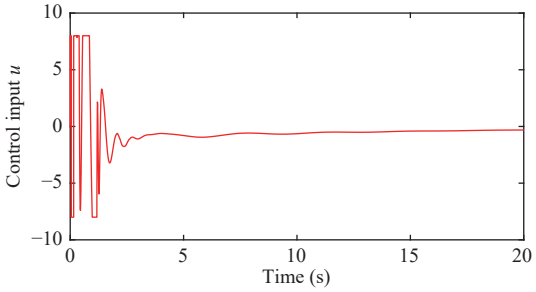

Fig. 7. Input signal u.

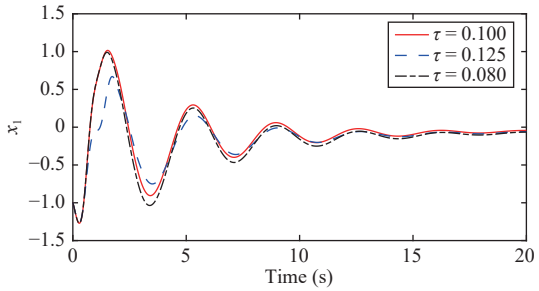

Fig. 8. System response with different ε.

VII. Conclusion and Future Work

In this paper, a predictor-based active disturbance rejection control (ADRC) is generalized to uncertain discrete-in-measurement nonlinear systems. The cases where the uncertain nonlinearity is not Lipschitz and the measurements are aperiodically sporadic have been investigated. The proposed control law comprises a novel extended state observer that is competent to estimate both system state and the total uncertainty without any interval. Theoretical analysis has shown the practical convergence of the closed-loop system. Simulations are carried out to illustrate the significance of the proposed design.

Some limitations of the proposed design include the limited estimation capability affected by sampling frequency, the problem of peaking during the transient period, and time delays. In future work, our research is thus divided into three aspects. First, we will attempt to develop the proposed ESO to a cascade form to accommodate larger sampling intervals. To address the problem of peaking, solutions such as selecting adaptive gains [36] can be utilized and need further investigation. Then, we will further explore the coupling effect of measurement discontinuity and measurement delay on our proposed controller.

Another topic comes from the fact that the ESO discussed in this paper is inevitably linear, and numerical studies [4] have shown that nonlinear ESOs perform very satisfactorily in convergence rate, robustness, and anti-chattering. Therefore, our future research work will focus on the practicability of general nonlinear ADRC for systems with intermittent measurements.

References

[1] Z. H. Zhao, J. Yang, S. H. Li, and W. H. Chen, "Composite nonlinear bilateral control for teleoperation systems with external disturbances," *IEEE/CAA J. Autom. Sinica*, vol. 6, no. 5, pp. 1220–1229, Sept. 2019.

Authorized licensed use limited to: TU Delft Library. Downloaded on February 02,2023 at 10:39:32 UTC from IEEE Xplore. Restrictions apply.

[2] X. J. Wang, Q. H. Wu, H. J. Wang, and X. H. Yin, "Adaptive neural tracking control for a class of non-lower triangular non-linear systems with dead zone and unmodelled dynamics," *IET Control Theory Appl.*, vol. 13, no. 5, pp. 672–682, Mar. 2019.

[3] Y. Z. Hua, X. W. Dong, Q. D. Li, and Z. Ren, "Distributed time-varying formation robust tracking for general linear multiagent systems with parameter uncertainties and external disturbances," *IEEE Trans. Cybern.*, vol. 47, no. 8, pp. 1959–1969, Aug. 2017.

[4] J. Q. Han, "From PID to active disturbance rejection control," *IEEE Trans. Ind. Electron.*, vol. 56, no. 3, pp. 900–906, Mar. 2009.

[5] K. H. He, C. Y. Dong, A. Yan, Q. Y. Zheng, B. Liang, and Q. Wang, "Composite deep learning control for autonomous bicycles by using deep deterministic policy gradient," in *Proc. 46th Annu. Conf. IEEE Industrial Electronics Society*, Singapore, 2020, pp. 2766−2773.

[6] L. Wang and J. B. Su, "Trajectory tracking of vertical take-off and landing unmanned aerial vehicles based on disturbance rejection control," *IEEE/CAA J. Autom. Sinica*, vol. 2, no. 1, pp. 65–73, Jan. 2015.

[7] Z. J. Zhao and Z. J. Liu, "Finite-time convergence disturbance rejection control for a flexible timoshenko manipulator," *IEEE/CAA J. Autom. Sinica*, vol. 8, no. 1, pp. 157–168, Jan. 2021.

[8] Z. Q. Gao, "Scaling and bandwidth-parameterization based controller tuning," in *Proc. American Control Conf.*, Denver, USA, 2003, pp. 4989–4996.

[9] S. Shao and Z. Gao, "On the conditions of exponential stability in active disturbance rejection control based on singular perturbation analysis," *Int. J. Control*, vol. 90, no. 10, pp. 2085–2097, May 2017.

[10] B. Z. Guo and Z. L. Zhao, "On the convergence of an extended state observer for nonlinear systems with uncertainty," *Syst. Control Lett.*, vol. 60, no. 6, pp. 420–430, Jun. 2011.

[11] Z. L. Zhao and B. Z. Guo, "A novel extended state observer for output tracking of mimo systems with mismatched uncertainty," *IEEE Trans. Autom. Control*, vol. 63, no. 1, pp. 211–218, Jan. 2017.

[12] T. T. Jiang, C. D. Huang, and L. Guo, "Control of uncertain nonlinear systems based on observers and estimators," *Automatica* , vol. 59, pp. 35–47, Sep. 2015.

[13] M. P. Ran, Q. Wang, C. Y. Dong, and L. H. Xie, "Active disturbance rejection control for uncertain time-delay nonlinear systems," *Automatica*, vol. 112, p. 108692, Feb. 2020. DOI: 10.1016/j.automatica.2019.108692.

[14] R. C. Roman, R. E. Precup, and E. M. Petriu, "Hybrid data-driven fuzzy active disturbance rejection control for tower crane systems," *Eur. J. Control*, vol. 58, pp. 373–387, Mar. 2021.

[15] Y. Y. Wang, X. X. Yang, and H. C. Yan, "Reliable fuzzy tracking control of near-space hypersonic vehicle using aperiodic measurement information," *IEEE Trans. Ind. Electron.* , vol. 66, no. 12, pp. 9439–9447, Dec. 2019.

[16] S. Suzuki, A. Isidori, and T. J. Tarn, "H_∞ control of continuous systems with sampled measurement," in *Proc. 33rd IEEE Conf. Decision and Control*, Lake Buena Vista, USA, 1994, pp. 2553−2558.

[17] P. Naghshtabrizi and J. P. Hespanha, "Designing an observer-based controller for a network control system," in *Proc. 44th IEEE Conf. Decision and Control*, Seville, Spain, 2005, pp. 848−853.

[18] T. Ahmed-Ali, R. Postoyan, and F. Lamnabhi-Lagarrigue, "Continuous-discrete adaptive observers for state affine systems," *Automatica*, vol. 45, no. 12, pp. 2986–2990, Dec. 2009.

[19] M. Nadri, H. Hammouri, and R. M. Grajales, "Observer design for uniformly observable systems with sampled measurements," *IEEE Trans. Autom. Control*, vol. 58, no. 3, pp. 757–762, Mar. 2012.

[20] T. N. Dinh, V. Andrieu, M. Nadri, and U. Serres, "Continuous-discrete time observer design for Lipschitz systems with sampled measurements," *IEEE Trans. Autom. Control*, vol. 60, no. 3, pp. 787–792, Mar. 2014.

[21] V. Andrieu, M. Nadri, U. Serres, and J. C. Vivalda, "Self-triggered continuous–discrete observer with updated sampling period," *Automatica*, vol. 62, pp. 106–113, Dec. 2015.

[22] G. L. Zhao and J. Mi, "Continuous-discrete adaptive observers for a class of nonlinear systems with sampled output," in *Proc. 36th Chinese Control Conf.*, Dalian, China, 2017, pp. 787−792.

[23] L. Etienne, L. Hetel, D. Efimov, and M. Petreczky, "Observer synthesis under time-varying sampling for Lipschitz nonlinear systems," *Automatica*, vol. 85, pp. 433–440, Nov. 2017.

[24] I. Karafyllis and C. Kravaris, "From continuous-time design to sampled-data design of observers," *IEEE Trans. Autom. Control* , vol. 54, no. 9, pp. 2169–2174, Sep. 2009.

[25] I. Bouraoui, M. Farza, T. Ménard, R. B. Abdennour, M. M'Saad, and H. Mosrati, "Observer design for a class of uncertain nonlinear systems with sampled outputs—application to the estimation of kinetic rates in bioreactors," *Automatica*, vol. 55, pp. 78–87, May 2015.

[26] T. Ahmed-Ali, E. Fridman, F. Giri, L. Burlion, and F. Lamnabhi-Lagarrigue, "Using exponential time-varying gains for sampled-data stabilization and estimation," *Automatica* , vol. 67, pp. 244–251, May 2016.

[27] D. Y. Zhang and Y. J. Shen, "Continuous sampled-data observer design for nonlinear systems with time delay larger or smaller than the sampling period," *IEEE Trans. Autom. Control* , vol. 62, no. 11, pp. 5822–5829, Nov. 2017.

[28] L. Etienne, L. Hetel, and D. Efimov, "Observer analysis and synthesis for perturbed Lipschitz systems under noisy time-varying measurements," *Automatica*, vol. 106, pp. 406–410, Aug. 2019.

[29] C. Tréangle, M. Farza, and M. M'Saad, "Filtered high gain observer for a class of uncertain nonlinear systems with sampled outputs," *Automatica*, vol. 101, pp. 197–206, Mar. 2019.

[30] O. Bernard, G. Sallet, and A. Sciandra, "Nonlinear observers for a class of biological systems: Application to validation of a phytoplanktonic growth model," *IEEE Trans. Autom. Control* , vol. 43, no. 8, pp. 1056–1065, Aug. 1998.

[31] H. B. Zhang, X. M. Liu, H. H. Ji, Z. S. Hou, and L. L. Fan, "Multi-agent-based data-driven distributed adaptive cooperative control in urban traffic signal timing," *Energies* , vol. 12, no. 7, p. 1402, Apr. 2019. DOI: 10.3390/en12071402.

[32] X. L. Tao, J. Q. Yi, Z. Q. Pu, and T. Y. Xiong, "Robust adaptive tracking control for hypersonic vehicle based on interval type-2 fuzzy logic system and small-gain approach," *IEEE Trans. Cybern.*, vol. 51, no. 5, pp. 2504–2517, May 2019.

[33] K. H. He, C. Y. Dong, and Q. Wang, "Active disturbance rejection adaptive control for uncertain nonlinear systems with unknown time-varying dead-zone input," *Asian J. Control*, 2021, DOI: 10.1002/asjc.2514.

[34] J. Lee, R. Mukherjee, and H. K. Khalil, "Output feedback stabilization of inverted pendulum on a cart in the presence of uncertainties," *Automatica*, vol. 54, pp. 146–157, Apr. 2015.

[35] Q. Zheng, L. Q. Gao, and Z. Q. Gao, "On validation of extended state observer through analysis and experimentation," *J. Dyn. Syst. Meas. Control*, vol. 134, no. 2, p. 024505, Mar. 2012. DOI: 10.1115/1.4005364.

[36] Z. Q. Pu, R. Y. Yuan, J. Q. Yi, and X. M. Tan, "A class of adaptive extended state observers for nonlinear disturbed systems," *IEEE Trans. Ind. Electron.*, vol. 62, no. 9, pp. 5858–5869, Sep. 2015.

[37] A. Benallegue, A. Mokhtari, and L. Fridman, "High-order sliding-mode observer for a quadrotor UAV," *Int. J. Robust Nonlinear Control*, vol. 18, no. 4–5, pp. 427–440, Mar. 2008.

[38] M. Fliess, R. Marquez, E. Delaleau, and H. Sira-Ramírez, "Correcteurs proportionnels-intégraux généralisés," *ESAIM*: *Control*, *Optimisation and Calculus of Variations*, vol. 7, pp. 23–41, Jan. 2002.

[39] L. B. Freidovich and H. K. Khalil, "Performance recovery of feedback-linearization-based designs," *IEEE Trans. Autom. Control* , vol. 53, no. 10, pp. 2324–2334, Nov. 2008.

[40] D. W. Shi, J. Xue, L. X. Zhao, J. Z. Wang, and Y. Huang, "Event-triggered active disturbance rejection control of DC torque motors," *IEEE/ASME Trans. Mechatron.*, vol. 22, no. 5, pp. 2277–2287, Oct.

Authorized licensed use limited to: TU Delft Library. Downloaded on February 02,2023 at 10:39:32 UTC from IEEE Xplore. Restrictions apply.

2017.

[41] J. K. Sun, J. Yang, S. H. Li, and W. X. Zheng, "Sampled-data-based event-triggered active disturbance rejection control for disturbed systems in networked environment," *IEEE Trans. Cybern.* , vol. 49, no. 2, pp. 556–566, Feb. 2019.

[42] M. P. Ran, Q. Wang, and C. Y. Dong, " Stabilization of a class of nonlinear systems with actuator saturation via active disturbance rejection control," *Automatica*, vol. 63, pp. 302–310, Jan. 2016.

[43] H. Omran, L. Hetel, M. Petreczky, J. P. Richard, and F. Lamnabhi-Lagarrigue, "Stability analysis of some classes of input-affine nonlinear systems with aperiodic sampled-data control," *Automatica* , vol. 70, pp. 266–274, Aug. 2016.

[44] A. Teel and L. Praly, "Tools for semiglobal stabilization by partial state and output feedback," *SIAM J. Control Optim.*, vol. 33, no. 5, pp. 1443–1488, Sep. 1995.

[45] H. K. Khalil, "Cascade high-gain observers in output feedback control," *Automatica*, vol. 80, pp. 110–118, Jun. 2017.

[46] K. H. He, C. Y. Dong, and Q. Wang, "Cascade integral predictors and feedback control for nonlinear systems with unknown time-varying input-delays," *Int. J. Control Autom. Syst.*, vol. 18, no. 5, pp. 1128–1138, May 2020.

[47] J. H. Ahrens and H. K. Khalil, "High-gain observers in the presence of measurement noise: A switched-gain approach," *Automatica* , vol. 45, no. 4, pp. 936–943, Apr. 2009.

[48] G. Phanomchoeng and R. Rajamani, " Observer design for Lipschitz nonlinear systems using Riccati equations," in *Proc. American Control Conf.*, Baltimore, USA, 2010, pp. 6060−6065.

Kanghui He (Student Member, IEEE) received the B.S. degree at the School of Mechanical Engineering and Automation, Beihang University, in 2018, and the M.S. degree in the Department of Flight Dynamics and Control, Beihang University, in 2021. He is now a Ph.D. candidate at the Delft Center for System and Control, Delft University of Technology, Delft, the Netherlands. His research interests include reinforcement learning based control, disturbance rejection control, hybrid systems, and their applications to robotics and transportation systems.

Chaoyang Dong is a Professor at the School of Aeronautic Science and Engineering, Beihang University. He received the Ph.D. degree in guidance, navigation and control in 1996 from Beihang University. He has authored or co-authored more than 100 papers. His research interests include multi-agent systems, distributed control, and modeling and synthesis of electrical systems.

Qing Wang is a Professor at the School of Automation Science and Electrical Engineering, Beihang University. She received the Ph.D. degree in flight control, guidance and simulation from Northwestern Polytechnical University, in 1996. She has authored or co-authored more than 150 papers. Her research interests include multi-agent systems, switch control, and fault detection.

Authorized licensed use limited to: TU Delft Library. Downloaded on February 02,2023 at 10:39:32 UTC from IEEE Xplore. Restrictions apply.